Anti Skid Control with Motor in Electric Vehicle

Shin-ichiro Sakai Hideo Sado Yoichi Hori

Department of Electrical Engineering, University of Tokyo
7-3-1 Hongo, Bunkyo, Tokyo, 113-8656, JAPAN
tel:+81-3-5841-7683; fax:+81-5841-7687; e-mail:sakai@hori.t.u-tokyo.ac.jp

Abstract: Motor's fast torque response is one remarkable advantage of electric vehicle (EV). Advanced anti skid control seems to be available with this advantage of EV. Simulation results pointed out that the feedback gain of wheel velocity control can be high enough to suppress the serious skid, if the actuator's delay is small enough. The dynamics of wheel can be changed with this control, and the driven wheel's inertia can be increased equivalently. Experiments results showed the effectiveness of this skid prevention method. This is the fast minor loop control of driven wheel, achieved only with the fast torque response of electric motor. Such method seems to be the appropriate way to maximize the advantage of EV.

1 Introduction

Electric Vehicle (EV) is evolving to be practical enough. Hybrid EV (HEV) like Toyota Prius is commercially succeeding, and Fuel cell EV (FCEV) will possibly be a major vehicle in the 21st century.

From the viewpoint of electric and control engineering, EV has remarkable advantages over conventional internal combustion engine vehicle(ICV). One of them is the fast and precise torque response of electric motor. This advantage suggests that more effective anti-skid brake system (ABS) or traction control system (TCS) should be available with EV.

In this paper, we compare the electric motor with hydraulic brake system, as an actuator of anti skid control. With simulations considering the delay of actuator response, the advantage of electric motor, fast torque response, is clarified. The control algorithm used in this comparison is based on the model following control (MFC) of driven wheel. In the latter part of this paper, MFC's effectiveness in the skid prevention is experimentally examined with our experimental EV. This method can increase the equivalent inertia of wheel, thus it makes the dynamics of slip phenomena relatively slow.

2 Conventional Brake and Electric Brake

In the conventional ICV, hydraulic brake system is generally used. The brake torque on each wheel depends on the hydraulic pressure of wheel cylinder. To control the hydraulic pressure, some solenoids are used. The connection of hydraulic circuitry can be switched with each solenoids position. The "2 position type" solenoid can change the hydraulic pressure, either to increase or to decrease. Another solenoid type has 3 status, for example, increasing, decreasing and holding the pressure.

One simple example is the ABS with 2 solenoids of 2 position type. The "main" solenoid changes the hydraulic circuitry, either to increase hydraulic pressure or to decrease it. The other "sub" solenoid switches the increasing/decreasing ratio either fast or slow.

In such hydraulic ABS system, delay in the response of the brake cylinder pressure is considerable. One source of this delay is the dead time of the solenoid. It is said to be more than some mili-seconds, for example 10 [ms] [1]. Another reason of the response delay is in the hydraulic circuitry, connecting the solenoids and the wheel cylinder. In results, the transfer function from the commanded hydraulic pressure value to the actual hydraulic pressure value at wheel cylinder may be expressed with dead time of 10-40[ms] and first order delay of 50-100[ms] [1].

On the other hand, regeneration brake is widely applied for the recent electric vehicles. In such EV, electric motor can be an actuator of ABS without any additional components. The time response of the electric motor is quite fast, such as 1[ms]. This quick torque response is achieved by the precise control of motor current. Typical sampling period of current control is less than 100 [μ s].

In the next part of this paper, the influence of such delay in the ABS system will be discussed with simulations. In these simulations, we describe the brake actuator as

$$G(s) = e^{-\tau_D s}\frac{1}{\tau_m s + 1}, \tag{1}$$

with 5 types of parameters in Table. 1.

	τ_D	τ_m
Type-I(electric motor)	100 [μs]	1[ms]
Type-II(hydraulic brake)	5 [ms]	50[ms]
Type-III(hydraulic brake)	10 [ms]	50[ms]
Type-IV(hydraulic brake)	20 [ms]	100[ms]
Type-V(hydraulic brake)	30 [ms]	100[ms]

Table 1: Modeling of ABS actuator

3 Slip phenomena and anti skid control

To discuss about the influence of actuator's delay in the ABS systems, here authors mention about the slip phenomena of wheel. Ordinary, slip ratio λ is used to evaluate the slip [1]. Slip ratio λ is defined as

$$\lambda = \begin{cases} \dfrac{V_w - V}{V_w} & : \text{accelerating wheel}, \\ \dfrac{V_w - V}{V} & : \text{deccelerating wheel}, \end{cases} \tag{2}$$

where V is the wheel absolute velocity or vehicle chassis velocity. V_w is the velocity equivalent value of wheel rotating speed,

$$V_w = r\omega, \tag{3}$$

where r, ω are the wheel radius and wheel rotating velocity, respectively.

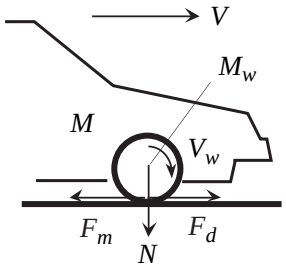

Fig.1: One wheel vehicle model.

Fig. 1 depicts the dynamics of wheel, where M is the vehicle weight. M_w is the mass equivalent value of wheel inertia J,

$$M_w = \frac{J}{r^2}. \tag{4}$$

F_m is the force equivalent value of accelerating or decelerating torque of actuator, generated by engine, wheel cylinder in the brake system or electric motor. F_d is the driving/braking force between the wheel and the road. This F_d has nonlinear dependence on the slip ratio λ. Here normalized traction force μ is defined as

$$\mu = \frac{F_d}{N}, \tag{5}$$

where N is the normal force on the wheel. Fig. 2 plots the examples of this normalized traction force μ vs. slip ratio.

With simple one wheel vehicle model (Fig. 1), the dynamic equations of wheel and chassis can be obtained as

$$M_w \frac{dV_w}{dt} = F_m - F_d(\lambda), \tag{6}$$

$$M \frac{dV}{dt} = F_d(\lambda), \tag{7}$$

[1] s is the most usual variable for slip ratio. However, we choose λ to distinguish it from the Laplace operator s.

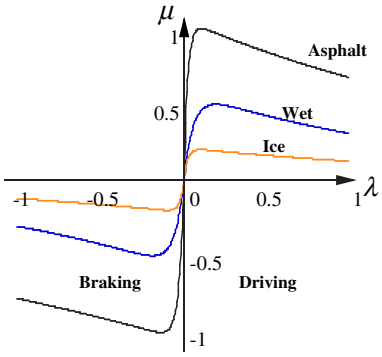

Fig.2: Typical $\mu - \lambda$ curves for various road conditions.

if air resistance on chassis and rotating resistance on wheel are both negligible.

When large torque rapidly generated on the wheel, or the F_d suddenly drops with road condition variation, wheel skid occurs. Slip ratio λ rapidly increases toward 1.0. With such large slip ratio, the driving/braking force F_d decreases as shown in Fig. 2. More serious problem is that, the side force generation on the wheel disappears with increasing slip ratio. This causes unstable vehicle lateral motion, such as dangerous spin motion.

Therefore, ABS was proposed and is widely used. Various method has been proposed for ABS [2] [3]. Conventional systems sense the acceleration of wheel velocity and/or slip ratio, and decrease or increase the wheel cylinder hydraulic pressure. Fig. 3 [4] shows the typical time response of chassis and wheel velocity. Note that V_{bx} and V_{wx} denote the chassis velocity and the wheel velocity, respectively. This is a control concept view of enhanced ABS with statistical analysis of road condition, however, large drop of wheel velocity appears at the beginning of control.

In the following part of this paper, we discuss about the ABS in the electric vehicle. However, our experimental vehicle has a series-wound DC motor and an one-quadrant chopper. It means that the electric brake is impossible with this vehicle. Therefore, the skid prevention for accelerating vehicle is studied in the following sections.

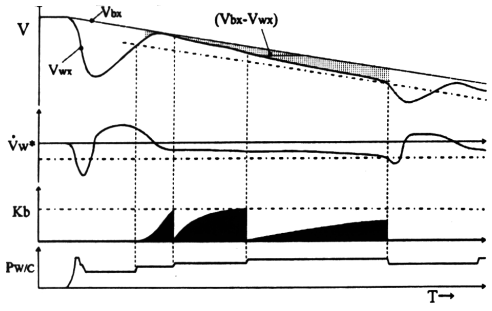

Fig.3: Typical time response of chassis velocity V_{bx} and wheel velocity V_{wx} [4].

4 The influence of actuator's delay in the anti skid control

As shown in Fig. 3, the wheel velocity drops when the wheel skid occurs with large torque input. This causes the rapid increase of slip ratio. Therefore, the feedback control of wheel velocity seems to be effective, to suppress the sharp increase of slip ratio. In this section, we discuss about the effect of wheel velocity control for skid prevention, especially about the influence of actuator's response delay.

4.1 Design of wheel velocity controller

For the design of wheel velocity controller, the strategy based on the two-degree-of-freedom control system is applied. Fig. 4 depicts the structure of two-degree-of-freedom control theory [5]. Here, u is the controller's output, r is the reference value, y is the output of plant, d is the disturbance and ξ is the observation noise. In this method, controller is determined with the design of command input response $G_{yr}(s)$ and sensitivity function $S(s)$. With $G_{yr}(s)$ and $S(s)$, the feedforward controller $C_1(s)$ and feedback controller $C_2(s)$ can be obtained as,

$$C_1(s) = \frac{G_{yr}(s)}{P_n(s)S(s)}, \tag{8}$$

$$C_2(s) = \frac{1-S(s)}{P_n(s)S(s)}, \tag{9}$$

where P_n is the nominal plant model. With these C_1 and C_2, the system can be modified into the block diagram as Fig. 5, where

$$d' = d(s) + \left(\frac{1}{P(s)} - \frac{1}{P_n(s)}\right) y(s). \tag{10}$$

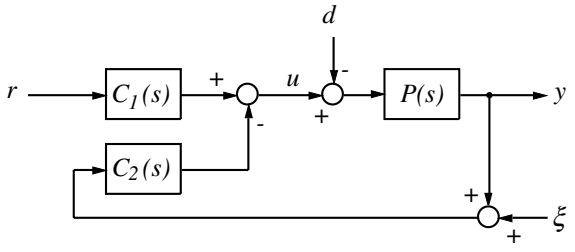

Fig.4: Two-degree-of-freedom control system.

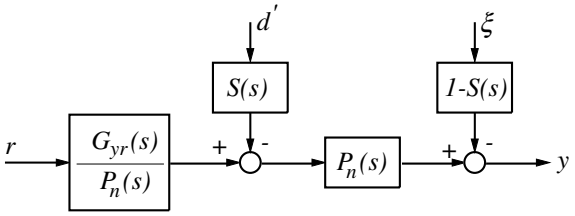

Fig.5: Equivalent block diagram of Fig. 5.

This controller is for skid prevention, hence the nominal plant model should be the model of adhesive wheel. With simple calculation based on the one wheel vehicle model (Fig. 1), the nominal model is chosen as,

$$P_n(s) = \frac{1}{(M+M_w)s}. \tag{11}$$

As commonly known, the sensitivity function $S(s)$ determine the disturbance rejection performance. In general case, $S(s)$ should have low gain in the low-frequency domain to suppress the disturbance or plant parameter fluctuation. In this section, $S(s)$ is selected as

$$S(s) = \frac{s^2}{(s+w_c)^2}. \tag{12}$$

Therefore, the parameter of controller is only w_c. Large w_c causes the high cut-off frequency of sensitivity function $S(s)$, and this indicates the strong disturbance rejection performance. In other words, high w_c means the high gain feedback controller.

The design of command input response $G_{yr}(s)$ is set to be

$$G_{yr}(s) = \frac{1}{\tau_{yr}s+1}, \tag{13}$$

however, command response is not so important in this paper. Thus the τ_{yr} is always 0.5[s] without any reasons.

4.2 Slip simulations with delay in the actuator response

Then some simulations are carried out for skid prevention with wheel velocity control. In these simulations, Magic Formula [6] is applied to calculate the nonlinear $\mu - \lambda$ curve. Parameters of Magic Formula are selected for $\mu - \lambda$ curve to have its peak value μ_{peak} at $\lambda = 0.1$. At 1.0[s], the command value of wheel speed starts to increase, with $dV_w/dt = 2[\text{m/s}^2]$. μ_{peak} is 0.75 at the beginning of this simulation, and at 3.0[s], μ_{peak} suddenly drops to 0.4. Without feedback control, serious wheel skid occurs as Fig. 6(a), with this sudden road condition variation.

If the actuator has no response delay, wheel velocity control with high w_c can be applied as in Fig. 6(b). The increase of slip ratio is relatively small or slow, compared to Fig. 6(a). Therefore, the lateral stability of vehicle can be enhanced. Fig. 7 shows the same simulation results with Type-IV actuator. The response comes to be unstable, with actuator response's delay.

Therefore, the w_c should be low enough to achieve stable response, if actuator delay exists. In this paper, the w_c is chosen for various types of actuator in the following methods:

1. Set w_c quit high, then decrease it until the simulation results comes to be stable.

2. Use the half value of this "limit" w_c.

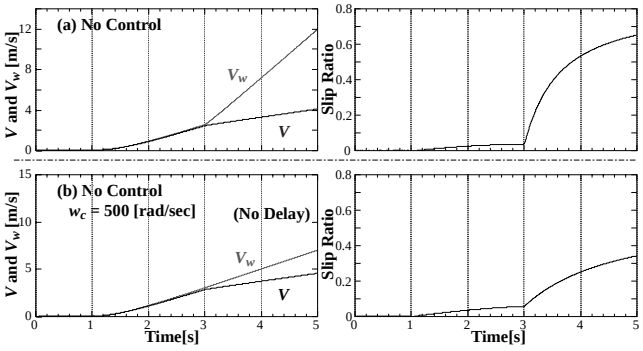

Fig.6: Simulation results, (a) without control and (b) with control.

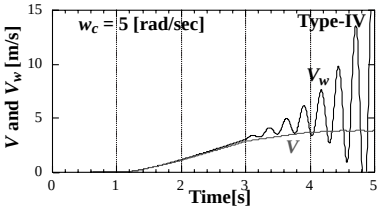

Fig.7: Simulation results with type-IV actuators and high w_c controller.

Fig. 8 shows the simulation results with type I∼V actuators and found maximum w_c. As Fig. 8 shows, the actuator response limits the w_c. With relatively small w_c, or with lower cut-off frequency of sensitivity function $S(s)$, the wheel velocity is disturbed more seriously with sudden road condition change at 3.0[s], then the slip ratio increases more rapidly. In these simulation, the wheel velocity is affected by

- drop of traction force F_d, ie., disturbance,
- and the plant fluctuation.

Note that once skid occurs, the plant changes from nominal plant $1/(M + M_w)s$ to $1/M_w s$. Therefore, the disturbance rejection performance is important for skid prevention.

These results indicate that, high cut-off frequency w_c such as 5 [rad/s] is required, to enhance the robustness of wheel velocity for slip phenomena. To apply such high w_c, dead time should be less than 5[ms]. It is not easy for hydraulic brake system. This seems to be the reason of the rapid change of wheel velocity in conventional ABS, as shown in Fig. 3. On the contrary, the response delay of electric motor can easily be less than 1[ms]. Accordingly, the cut-off frequency of sensitivity function or the feedback gain can be high enough. This is the primal advantage of electric motor in ABS or TCS systems.

5 Skid prevention experiments with wheel velocity control (MFC)

Model following control (MFC) of wheel velocity was proposed for EV [7]. Fig. 9 shows the block diagram of MFC. With Fig. 9, the sensitivity function can be calculated as

$$S(s) = \frac{s+a}{s+b}, \tag{14}$$

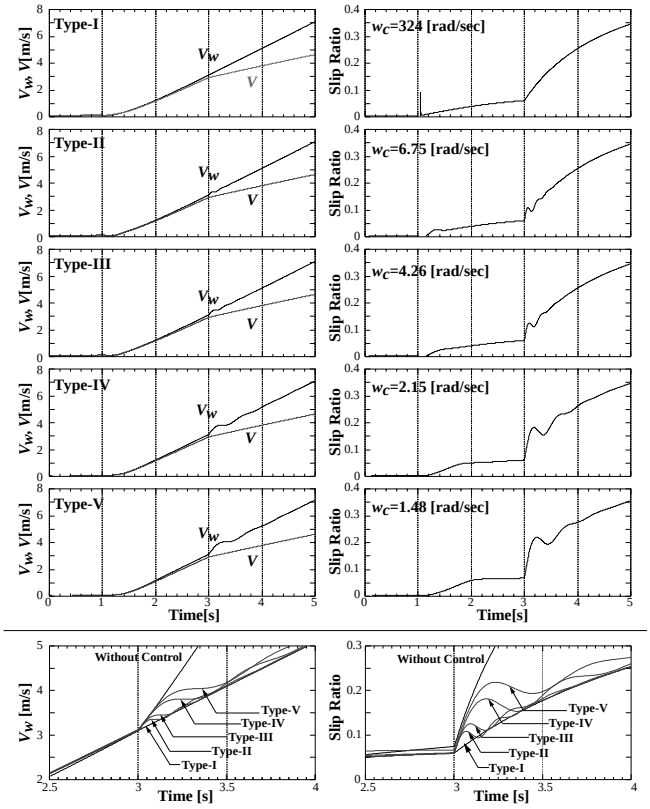

Fig.8: Simulation results with control and type-I∼V actuators.

where

$$a = \frac{M + (1 - K_p)M_w}{(M + M_w)\tau}, \tag{15}$$

$$b = \frac{(1 + K_p)M + M_w}{(M + M_w)\tau}. \tag{16}$$

K_p, τ are the feedback gain and time constant of MFC. Since $a < b$, the bode diagram of (14) is as Fig. 10. As this figure shows, the difference between the simple wheel velocity controller's sensitivity functions and MFC's $S(s)$ is the gain in the low-frequency domain. Generally, This cause the steady state error for disturbance. It is an undesirable performance for general servo system, however, not so for skid avoidance. Important performance is to prevent the rapid increase of slip ratio, and strict control of wheel velocity is not required at all.

Experiments of MFC with low μ road were carried out in this paper with our experimental EV, "UOT Electric March-I". The configuration of this vehicle is depicted in Fig. 11, and its specification is appeared in Table 2. As mentioned above, this vehicle has series-wound DC motor and one quadrant chopper, and regeneration brake is not available.

To examine the effect of MFC in skid avoidance, slippery low μ road is required. We put the aluminum plates of 14[m] length on the asphalt, as Fig. 12, and spread water on these plates. The peak μ of this test road is about 0.5. This value was estimated based on some experimental results.

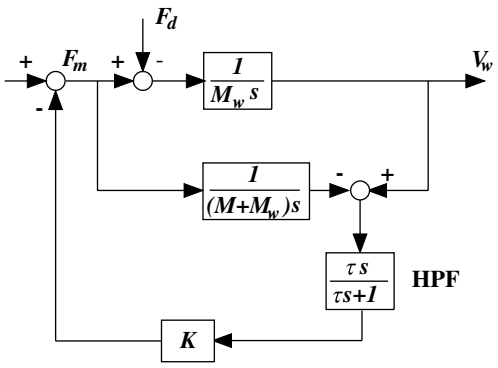

Fig.9: Block Diagram of MFC.

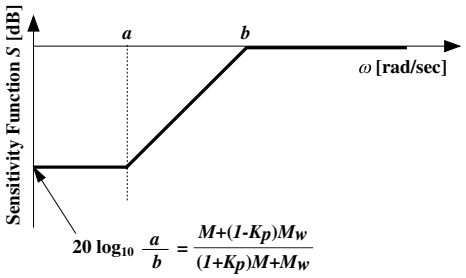

Fig.10: Sensitivity function $S(s)$ of MFC.

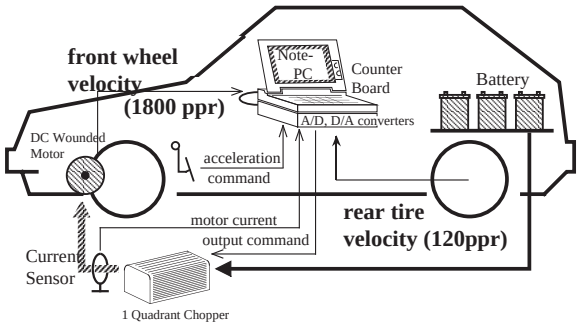

Fig.11: Configuration of "UOT Electric March-I".

Motor	**DC Motor**
Rated Power(5 min.)	32.5[kW] (44.3[HP])
Max. Torque	85[Nm]
Gear Ratio	13.5
Battery	**Lead Acid**
Nominal Capacity	92[Ah]
Total Voltage	120[V] (with 10 units)
Chassis	**Nissan March**
Weight	1000[kg]
Wheel Inertia	21.1[kgm^2]*
Wheel Radius	0.26[m]
CPU	**i386, 20[MHz]**
Encoder(front/rear)	1800/120[ppr]

* ... Including the rotor of motor, affected by gear ratio.

Table 2: Specifications of "UOT Electric March I".

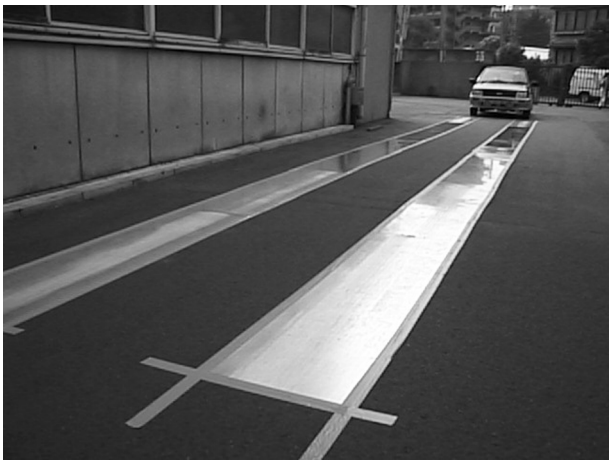

Fig.12: Slippery test road and "UOT Electric March-I".

Fig. 13 shows the experimental results of MFC, comparing them with simulation results. In these experiments, vehicle accelerated on the slippery test road, with lineally increasing motor torque. Without MFC ($K_p = 0$), the slip ratio rapidly increases. The battery voltage is not high enough, hence the acceleration of wheel velocity decreases at 3.0[s]. The vehicle reached the end of the 14[m] low μ road at 5.5[s], then ran again on the dry asphalt road. Thus the slip ratio rapidly decreases even without feedback control after 5.5[s].

On the contrary, the increase of slip ratio is relatively slow with MFC. As Fig. 13 shows, the wheel velocity is insensitive to the slip status, if the feedback gain K_p is high enough, such as 5 or 10. Fig. 14 shows this MFC effect with comparison of slip ratios.

The effect of such wheel velocity control can be expressed as: "changing the wheel dynamics with feedback control". The controller, designed in section 4.1 or MFC, can increase the wheel's inertia equivalently. This changes the dynamics of slip phenomena.

To evaluate this effect, here the perturbation systems of (6), (7) and $\mu(\lambda)$ curve are described as,

$$M_w \Delta \dot{V} = \Delta F_m - \Delta F_d, \tag{17}$$

$$M \Delta \dot{V}_w = \Delta F_d, \tag{18}$$

$$\Delta F_d = a \Delta \lambda. \tag{19}$$

With these equations, transfer function from motor torque F_m to slip ratio λ can be calculated as,

$$\frac{\Delta \lambda}{\Delta F_m} = \frac{1}{aN} \frac{M(1-\lambda_0)}{M(1-\lambda_0)+M_w} \frac{1}{\tau_a s + 1}, \tag{20}$$

where

$$\tau_a = \frac{M_w V_{w0}}{aN} \frac{M}{M(1-\lambda_0)+M_w}, \tag{21}$$

for the vehicle without control. λ_0 and V_{w0} is the slip ratio and wheel velocity at the approximated point, respectively. a is the gradient of $\mu - \lambda$ curve at this approximated point, as (19).

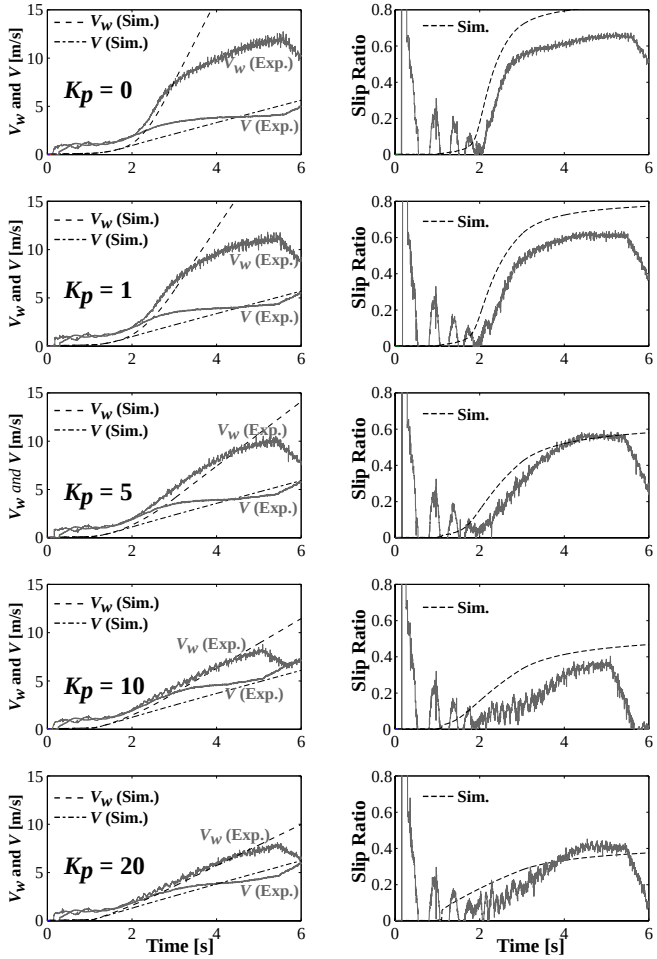

Fig.13: Slip experimental results of MFC.

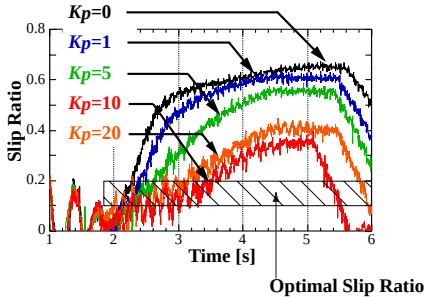

Fig.14: MFC effect of slip prevention.

If the MFC effect is the ideal one, the wheel inertia seems to be $1/(M + M_w)$. Therefore, the slip dynamics changes to be

$$\frac{\Delta\lambda}{\Delta F_m} = \frac{1}{aN}\frac{M(1-\lambda_0)}{M+M_w}\frac{1}{\tau_a{}'s}, \tag{22}$$

where

$$\tau_a{}' = \frac{MV_{w0}}{aN}. \tag{23}$$

As these equation shows, the original slip time constant τ_a is increased to τ_a' as

$$\frac{\tau_a{}'}{\tau_a} = 1 + \frac{M}{M_w}(1-\lambda_0), \tag{24}$$

with wheel velocity control such as MFC. This effect, slip time constant enlargement, depends on the ratio of vehicle weight M and wheel inertia M_w, as (24) shows. For our experimental vehicle, the value of τ_a'/τ_a is 4.5. Fig. 13 indicates that the slip ratio grew as 5 times as slowly with MFC of $K_p = 10$ or 20, pointing out that the estimation described above was appropriate.

6 Conclusion

In this paper, the electric motor was compared with hydraulic brake system as an ABS actuator. Simulation results pointed out that, the feedback gain could not be high enough to prevent the rapid change of wheel velocity, if the actuator's delay is considerable. The delay in the hydraulic brake system seems to be such limitation. Electric motor's torque response is much faster, therefore, more effective ABS will be available. Thus the ABS in EV should be actuated by electric motor.

In the latter part of this paper, experiments was carried out with MFC, which is a method of wheel velocity control. MFC was effective to suppress the rapid increase of slip ratio. Note that the conventional ABS is based on the slip ratio, thus it requires the value of chassis velocity, however, it can not be measured or estimated easily. On the contrary, methods like MFC requires only the wheel velocity, and can change the dynamics of driven wheel or slip phenomena. Such fast minor loop control seems to be the appropriate way to maximize the advantage of EV, fast motor torque response.

The MFC can prevent the sudden change of wheel velocity, however, it cannot prevent skid completely. Fig. 13 shows it clearly. Even the wheel velocity was controlled to be nominal, slip ratio still increased with the change of chassis velocity. Thus chassis velocity estimation or wheel skid detection is required for complete skid prevention. In EV, wheel skid can be detected without chassis velocity[8]. Cooperation of wheel velocity control and such method still remains for further studies.

References

[1] T. Tabe, N. Ohka, H. Kuraoka, and M. Ohba, "Automotive antiskid system using modern control theory," in *Proc. IEEE IECON'85*, pp. 390–395, 1985.

[2] T. Kawabe, M. Nakazawa, I. Notsu, and Y. Watanabe, "A sliding mode controller for wheel slip ratio control system," in *Proc. AVEC'96*, pp. 797–804, 1996.

[3] Salman MA, "A robust servo-electronic controller for brake force distribution," *Trans. of ASME Dynamic Systems, Measurement, and Control*, vol. 112, no. 3, pp. 442–227, 1990.

[4] Y. Imoto, N. Tsuru, M. Imaeda, T. Watanabe, and S. Masaki, "High-efficiency brake pressure controls in ABS," in *AVEC '98*, pp. 655–660, 1998.

[5] Y. Fujimoto and A. Kawamura, "Robust servo-system based on two-degree-of-freedom control with sliding mode," *IEEE Trans. Ind. Applicat.*, vol. 42, no. 3, pp. 272–280, 1995.

[6] H. B. Pecejka and E. Bakker, "The Magic Formula tyre model," in *Proc. 1st International Colloquium on Tyre Models for Vehicle Dynamics Analysis*, 1991.

[7] Y. Hori, Y. Toyoda, and Y. Tsuruoka, "Traction control of electric vehicle: Basic experimental results using the test EV "UOT electric march"," *IEEE Trans. Ind. Applicat.*, vol. 34, no. 5, pp. 1131–1138, 1998.

[8] S. Sakai, H. Sado, and Y. Hori, "Novel skid avoidance method for electric vehicle with independently controlled 4 in-wheel motors," in *Proc. IEEE ISIE'99* pp. 934–939, 1999.